Palaeontologia Electronica
http://palaeo-electronica.org

AN INDEX FOR CONCAVITY OF THE OCCLUSAL SURFACE OF THE CHEEK TEETH AND AN ASSESSMENT OF CONCAVITY IN GLIRIDAE (MAMMALIA, RODENTIA)

Matthijs Freudenthal and Elvira Martín-Suárez

ABSTRACT

Many studies of fossil Gliridae have found that the concavity of the occlusal surface is an important diagnostic character. However, no objective measure of occlusal concavity exists. In this paper a quantitative concavity index is proposed and tested on the glirid dentition. It may be applicable to other taxa, too.

The index is based on the depth of concavity and the radius of a best-fit circle. We drew anterior and posterior profiles of upper and lower M1 and M2 of over 60 species of Gliridae. These diagrams were digitized, after which six parameters were measured on each profile. We then calculated the radius of the circle that best fits each profile. The depth of the concavity divided by the radius of the best fitting circle was found to be a good measure of concavity. This parameter permits us to quantify descriptive terms like “weakly concave,” “moderately concave,” or “strongly concave.”

The oldest Gliridae, from the late Eocene, have moderately to strongly concave molars. During the late Oligocene various groups of Gliridae developed weakly concave or almost flat molars.

Matthijs Freudenthal. Departamento de Estratigrafía y Paleontología, Facultad de Ciencias, Campus Fuentenueva, Granada, Spain; Nationaal Natuurhistorisch Museum, Postbus 9517, 2300 RA Leiden, The Netherlands. mfreuden@ugr.es
Elvira Martín-Suárez. Departamento de Estratigrafía y Paleontología, Facultad de Ciencias, Campus Fuentenueva, Granada, Spain. elvirams@ugr.es

KEY WORDS: Gliridae; dental concavity

INTRODUCTION

In the course of a revision of the fossil glirid genera *Bransatoglis* and *Microdyromys*, we observed that many authors consider the concavity of the occlusal surface to be an important diagnostic character, e.g., de Bruijn (1967), Hugueney (1967), Bahlo (1975), van der Meulen and de Bruijn (1982), Daams and de Bruijn (1995), and Vianey-Liaud (2004). However, these descriptions were based on subjective assessments of how

PE Article Number: 10.2.9A

Submission: 8 January 2007. Acceptance: 9 July 2007

Freudenthal, Matthijs, and Martín-Suárez, Elvira, 2007. An Index for Concavity of the Occlusal Surface of the Cheek Teeth and An Assessment of Concavity in Gliridae (Mammalia, Rodentia). *Palaeontologia Electronica* Vol. 10, Issue 2; 9A:24p, 1.3MB;
http://palaeo-electronica.org/paleo/2007_2/00122/index.html

concave the surface is, assessments which are not very precise and which may vary from author to author. In this paper, we develop a quantification of concavity, which can serve as a diagnostic tool that reveals contradictions about concavity.

For example, Hugueney (1967) described the species *Bransatoglis concavidens*, characterizing it as having a very strongly concave occlusal surface on M^2, and Bahlo (1975) described *Oligodyromys planus* as having a weakly concave surface on the upper and lower dentitions. Later authors considered *Oligodyromys* to be a junior synonym of *Bransatoglis.* Our comparison of the surfaces of the upper molars of these two species using a new quantitative index showed no appreciable difference in concavity. In another example, Daams and de Bruijn (1995) defined the occlusal surface of the Dryomyinae as concave, and that of the Bransatoglirinae as strongly concave; however, when we compare *Eliomys quercinus*, as an example of the Dryomyinae with the holotype of *Bransatoglis concavidens*, one is inclined to say that the occlusal surface of *Eliomys quercinus* is more strongly concave than that of *Bransatoglis.*

Our measure of concavity is relatively simple and can be applied to any structure that has an irregularly concave cross-sectional profile. We drew profiles of the teeth of many glirid species, we measured several parameters on the digitized profiles, and we used those parameters to find the radius of a circle that best fit the entire concavity. We applied our index to a wide variety of glirid species to give a picture of the degree of concavity across the group, including a general assessment of trends in concavity from the Eocene to the Oligocene.

MATERIAL

Our material consisted of lower and upper M1 and M2 of over 60 species of Gliridae, as specified in Table 1. Most of the material is from the collections of the National Museum of Natural History, Leiden (Netherlands), and from the collections we are currently studying that will be deposited in the museum of the Earth Sciences Department of the University of Zaragoza (Spain). A very important contribution to our material was the 'collection Mein' in Lyon (France). In a few cases we used published or unpublished figures, made by other people.

Table 1 lists the species analyzed in this paper using a taxonomy based on the classification by Daams and de Bruijn (1995). We made some modifications to the taxonomy as follows: (1) Glamyinae are separated from the Gliravinae, as proposed by Vianey-Liaud (1994); (2) the Bransatoglirinae are divided into three groups, as proposed by Freudenthal and Martín-Suárez (in press), with the early Oligocene species attributed to *Oligodyromys*, the large species from the late Oligocene and Miocene attributed to *Bransatoglis* or *Paraglis*, and a third group formed by *Microdyromys*; and (4) *Stertomys* is placed in the Myomiminae, as proposed by Freudenthal and Martín-Suárez (2006).

The catalogue numbers of the specimens, as far as available, are listed in Table 2. Catalogue numbers with the code RGM belong to the National Museum of Natural History, Leiden (the Netherlands). The majority of the other catalogue numbers is based on one of the locality codes listed in Table 3. These specimens will be deposited in the Earth Sciences Department of the University of Zaragoza (Spain). 'Coll. Mein' refers to unnumbered specimens in the Mein collection, in many cases casts of original material.

Published figures were taken from: Bahlo (1975), *O. planus* from Heimersheim; Hugueney (1969), *P. fugax* from Coderet; Vianey-Liaud (2004), *G. antiquus* from Itardies.

METHODS

The three mentioned groups of Bransatoglirinae, and the Dryomyinae, Glamyinae, Gliravinae, Glirinae, and Myomiminae form the eight groups for which concavity will be compared.

We drew over 500 profiles in anterior and posterior view of lower and upper M1 and M2 of the available specimens of M_1, M_2, M^1, and M^2 with a camera lucida mounted on a Wild M8 or Wild M5 binocular microscope, normally at 50x magnification, but at 25x for the largest specimens.

Instead of using lengthy terms like 'anterior profile of M_1', 'posterior profile of M^2' we will use descriptive names for the eight profile classes: m1inf_ant, m1inf_post, m2inf_ant, m2inf_post, m1sup_ant, m1sup_post, m2sup_ant, and m2sup_post.

The anterior profile of the upper molars was drawn over the paracone and the anterior corner of the protocone, which are the most characteristic points of the profile in anterior view. Similarly, the posterior profile was drawn over the metacone and the posterior corner of the protocone. In the lower molars the metaconid and protoconid define the anterior view, and the entoconid and hypoconid the posterior view. In other words the curves do not

Table 1. Taxa included in this study. (Continued on next page.)

Group	Species Analyzed	Original Genus
Oligodyromys **(group 1)**	*Oligodyromys attenuatus* (Peláez-Campomanes 2000)	*Bransatoglis*
	Oligodyromys libanicus (Freudenthal and Martín-Suárez, in press)	*Oligodyromys*
	Oligodyromys parvus (Freudenthal 1996)	*Bransatoglis*
	Oligodyromys planus (Bahlo 1975)	*Oligodyromys*
	Oligodyromys sjeni (Ünay 1989)	*Bransatoglis*
Bransatoglis Paraglis **(group 2)**	*Paraglis astaracensis* (Baudelot 1970)	*Paraglis*
	Bransatoglis cadeoti (Bulot 1978)	*Bransatoglis*
	Bransatoglis concavidens (Hugueney 1967)	*Bransatoglis*
	Paraglis fugax (Hugueney 1967)	*Pseudodryomys*
	Paraglis infralactorensis (Baudelot and Collier 1982)	*Paraglis*
Microdyromys **(group 3)**	*Microdyromys misonnei* (Vianey-Liaud 1994)	*Bransatoglis*
	Microdyromys complicatus (de Bruijn 1966a)	*Microdyromys*
	Microdyromys legidensis (Daams 1981)	*Microdyromys*
	Microdyromys praemurinus (Freudenberg 1941)	*Dryomys*
Dryomyinae (group 4)	*Dryomys apulus* (Freudenthal and Martín-Suárez 2006)	*Dryomys*
	Dryomys nitedula (Pallas 1778)	*Mus*
	Eliomys intermedius (Friant 1953)	*Eliomys*
	Eliomys quercinus (Linnaeus 1766)	*Mus*
	Eliomys truci (Mein and Michaux 1970)	*Eliomys*
	Hypnomys morpheus (Bate 1918)	*Hypnomys*
	Maltamys wiedincitensis (Zammit Maempel and de Bruijn 1982)	*Maltamys*
	Paraglirulus agelakisi (Van der Meulen and de Bruijn 1982)	*Paraglirulus*
	Paraglirulus conjunctus (Mayr 1979)	*Paraglirulus*
Glamyinae (group 5)	*Glamys devoogdi* (Bosma and de Bruijn, 1979)	*Gliravus*
	Glamys nov. sp. (Freudenthal 2004)	*Glamys*
	Glamys olallensis (Freudenthal 1996)	*Glamys*
	Glamys priscus (Stehlin and Schaub 1951)	*Gliravus*
	Glamys robiacensis (Hartenberger 1965)	*Gliravus*
	Glamys umbriae (Freudenthal 2004)	*Glamys*

represent the anterior or posterior border, respectively, of the tooth. The shape and height of anteroloph(id) and posteroloph(id) may vary considerably within a sample, and should not be used to define the concavity of a specimen. In Figure 1 the location of the profiles in the occlusal surface is indicated. It also makes clear why the anteroloph is not suitable to define concavity.

Most of the computational work might have been performed using commercial computer programs, but in view of the large amount of data to be processed we decided to write a set of programs in Visual Basic. One of these programs allows the tracing of bitmaps (raster images). It converts the bitmaps into vector images by creating lines that connect the dots of a bitmap, and then it converts the vectors into a polygon. Once the polygon is created, a second program serves to calculate a standard set of parameters through the methods of analytic geometry, and a third one performs many comparisons of these parameters.

The drawings, as well as the published figures, were scanned, and the resulting bitmaps were oriented so that the occlusal side faced down. The figure was inverted if necessary so that the protocone/protoconid side faced left. This stan-

Table 1 (continued).

Gliravinae (group 6)	*Butseloglis bravoi* (Hugueney, Adrover, and Moissenet 1985)	*Gliravus*
	Butseloglis bruijni (Hugueney 1967)	*Gliravus*
	Butseloglis itardiensis (Vianey-Liaud 1989)	*Gliravus*
	Butseloglis micio (Misonne 1957)	*Peridyromys*
	Butseloglis montisalbani (Freudenthal 2004)	*Schizogliravus*
	Gliravus majori (Stehlin and Schaub 1951)	*Gliravus*
Glirinae (group 7)	*Glirudinus antiquus* (Vianey-Liaud 2004)	*Glirudinus*
	Glirudinus glirulus (Dehm 1935)	*Myoxus*
	Glirudinus modestus (Dehm 1950)	*Glirulus*
	Glis guerbuezi (Ünay 1989)	*Glis*
	Glis sackdillingensis (Heller 1930)	*Myoxus*
Myomiminae (group 8)	*Altomiramys daamsi* (Díaz and López 1979)	*Altomiramys*
	Armantomys aragonensis (de Bruijn 1966a)	*Armantomys*
	Armantomys parsani (Daams 1990)	*Armantomys*
	Armantomys tricristatus (López 1977)	*Armantomys*
	Dryomimus eliomyoides (Kretzoi 1959)	*Dryomimus*
	Myomimus dehmi (de Bruijn 1966b)	*Peridyromys*
	Nievella mayri (Daams 1976)	*Nievella*
	Peridyromys jaegeri (Aguilar 1974)	*Peridyromys*
	Peridyromys murinus (Pomel 1853)	*Myoxus*
	Praearmantomys crusafonti (de Bruijn 1966a)	*Praearmantomys*
	Prodryomys brailloni (Thaler 1966)	*Dryomys*
	Prodryomys gregarius (Dehm 1950)	*Dryomys*
	Pseudodryomys aguirrei (Adrover 1978)	*Pseudodryomys*
	Pseudodryomys ibericus (de Bruijn 1966a)	*Pseudodryomys*
	Pseudodryomys simplicidens (de Bruijn 1966a)	*Pseudodryomys*
	Stertomys daamsi (Freudenthal and Martín-Suárez 2006)	*Stertomys*
	Stertomys daunius (Freudenthal and Martín-Suárez 2006)	*Stertomys*
	Stertomys laticrestatus (Daams and Freudenthal 1985)	*Stertomys*
	Stertomys lyrifer (Martín-Suárez and Freudenthal 2007)	*Stertomys*
	Stertomys simplex (Martín-Suárez and Freudenthal 2007)	*Stertomys*
	Tempestia hartenbergeri (de Bruijn 1966b)	*Eliomys*
	Vasseuromys autolensis (Cuenca 1985)	*Ebromys*
	Vasseuromys duplex (Ünay 1994)	*Vasseuromys*

dardized orientation facilitates automatic computation. Then the bitmaps were vectorized (converted into polygons), and the polygons were exported to files in Hewlett Packard Graphics Language (HPGL) format. The number of vertices (**v**) in the occlusal concavity part of the polygon was chosen to lie between 15 and 20.

After this, the profiles were analyzed, parameters were calculated for each one, text labels were associated with the image, and the results were written to a text file.

Results for each of the eight profile classes (two profiles for each first and second molar, upper and lower) were compiled into a single text file that served as input to the next program that performed the comparisons of the parameters within profile classes and between profile classes, and which also produced graphic representations of the results.

The Parameters

The parameters are indicated in Figure 2: **w** is the maximum width of the molar as seen in the profile, **x** and **y** are the limits of the occlusal concavity: the top of the protocone, paracone, metacone, protoconid, metaconid, hypoconid, or entoconid, depending on the element in question, and the direction of the view. The letter **b** (base) designates

Table 2. Specimens included in this study. Locality codes in Table 3. (Continued on next page.)

Species	Locality	M_1	M_2	M^1	M^2
Oligodyromys					
O. attenuatus	AGT2D	RGM 455732	AGT2D 455	AGT2D 870	AGT2D 879
O. libanicus	MLB8	MLB8 1182	MLB8 1205	MLB8 1284	MLB8 1323
O. libanicus	MLB3Y	MLB3Y 139	MLB3Y 152	MLB3Y 180	MLB3Y 184
O. parvus	OLA4A	OLA4A 920	RGM 455543	OLA4A 1141 RGM 418108	RGM 455567
O. planus	HB				RGM 148893 RGM 148899
O. planus	HEIM		cast		Bahlo, Figure 37
O. planus	SMC				Figure Hugueney
O. sjeni	KOC	Coll. Mein	coll. Mein	coll. Mein	coll. Mein
Bransatoglis Paraglis					
B. cadeoti	BEZ		coll. Mein	coll. Mein	coll. Mein
B. concavidens	COD	Lyon 96253	cast		Hugueney unpubl; cast
P. astaracensis	SS	Coll. Mein	coll. Mein	coll. Mein	coll. Mein
P. astaracensis	POV			coll. Mein	
P. fugax	COD		cast		Hugueney Figure 80a; Hugueney unpubl.; cast
P. infralactorensis	Cocument	Coll. Mein			coll. Mein
Microdyromys					
M. complicatus	ARM7	Coll. Mein	coll. Mein		coll. Mein
M. complicatus	LGM	Coll. Mein	coll. Mein	coll. Mein	coll. Mein
M. legidensis	RA1	RGM 390731	RGM 390737	RGM 390739	RGM 390743
M. misonnei	MLB1D	MLB1D 1420	MLB1D 1430	MLB1D 1458 MLB1D 1461	MLB1D 1480 MLB1D 1482
M. misonnei	HB	RGM 148912	RGM 148917	RGM 148935	RGM 148815 RGM 148937
M. praemurinus	MIR1	RGM 417652	RGM 417663	MIR1 201	RGM 417699
M. praemurinus	VIV	RGM 418000	RGM 418018	VIV 367	VIV 396 RGM 418068
Dryomyinae					
D. apulus	BIA1		RGM 455927	RGM 455956	RGM 455963
D. nitedula	Ajeyrd			Lyon 38837	Lyon 38837
E. intermedius	BAL2	Coll. Mein	coll. Mein	coll. Mein	coll. Mein
E. quercinus	Darro	Recent	Recent	Recent	Recent
E. truci	HAU	Coll. Mein	coll. Mein		coll. Mein
H. morpheus	BAUZA	Coll. Mein	coll. Mein	coll. Mein	coll. Mein
M. wiedincitensis	Ghar-Dalam	Coll. Mein	coll. Mein		coll. Mein
P. agelakisi	ALI1	Coll. Mein	coll. Mein	coll. Mein	coll. Mein
P. conjunctus	SS	Coll. Mein		coll. Mein	coll. Mein
Glamyinae					
G. devoogdi	HB	RGM 148772	RGM 148781	RGM 148818	RGM 148820
G. olallensis	OLA4A	OLA4A 810	OLA4A 822	RGM 418618	OLA4A 866
G. priscus	AGT2D	AGT2D 397	AGT2D 409	AGT2D 606	AGT2D 431
G. robiacensis	Robiac	Coll. Mein	coll. Mein	coll. Mein	coll. Mein

Table 2 (continued).

G. umbriae	UMB1B	UMB1B 9	UMB1B 35	UMB1B 49	UMB1B 53
Glamys sp.	UMB1B		UMB1B 115	UMB1B 118	UMB1B 69
Gliravinae					
B. bravoi	VIV	VIV 450	VIV 452	VIV 479	VIV 493
B. bruijni	MIR4C	MIR4C 1160	MIR4C 1161		
B. bruijni	MIR4D			MIR4D 2091	MIR4D 2095 MIR4D 2093
B. itardiensis	OLA4A	RGM 386525	RGM 386593	OLA4A 1036	OLA4A 1065
B. micio	HB	RGM 148836	RGM 148846	RGM 148873	RGM 148878
B. montisalbani	MLB1D	MLB1D 1072	MLB1D 1113	MLB1D 1263	MLB1D 1316
G. majori	MIR4C	MIR4C 1028	MIR4C 1047	MIR4C 1100	MIR4C 1106
Glirinae					
G. antiquus	ITD		V-L: Figure 3cc4		V-L: Figure 2j3, 2u3
G. glirulus	COD		cast	cast	Lyon 96266 - 3
G. modestus	BN2	RGM 336446	RGM 268512	RGM 336437	RGM 336440
G. modestus	BOU1			coll. Mein	coll. Mein
G. modestus	OCE2C			OCE2C 2	
G. guerbuezi	KOC	Coll. Mein	coll. Mein	coll. Mein	coll. Mein
G. sackdillingensis	KAM	Coll. Mein			coll. Mein
Myomiminae					
A. daamsi	RA1	RGM 392879	RGM 392084	RGM 336031	RGM 336050
A. aragonensis	RA1				RGM 337789
A. parsani	RA1	RGM 337680		RGM 337765	RGM 337804
A. tricristatus	ESC	Coll. Mein	coll. Mein		coll. Mein
D. eliomyoides	TRK	Coll. Mein	coll. Mein	coll. Mein	coll. Mein
M. dehmi	NO2	RGM 195543	RGM 195544	RGM 195541	RGM 195542
N. mayri	CET		coll. Mein	coll. Mein	
P. jaegeri	LAU			coll. Mein	
P. murinus	RA1	RGM 195548	RGM 195549	RGM 195550	RGM 195551
P. murinus	VIV	RGM 417949	RGM 417953	RGM 417968	RGM 417977
P. crusafonti	NAV	Coll. Mein	coll. Mein		coll. Mein
P. brailloni	BOU1	Coll. Mein	coll. Mein	coll. Mein	coll. Mein
P. gregarius	WW	Coll. Mein	coll. Mein	coll. Mein	coll. Mein
P. aguirrei	NAV	Coll. Mein	coll. Mein	coll. Mein	coll. Mein
P. ibericus	RA1	RGM 336017	RGM 336023	RGM 336049	RGM 336001
P. simplicidens	RA1	RGM 195552	RGM 195553	RGM 195554	RGM 195555
S. daamsi	BIA1	RGM 513882	RGM 513932	RGM 455811	RGM 386882
S. aff. *daamsi*	RIN1	RGM 514237	RGM 514272	RGM 535091	RGM 535123
S. daunius	BIA1	RGM 514143	RGM 514149	RGM 514174	RGM 514180
S. laticrestatus	SG	RGM 258175	RGM 258180	RGM 258176	RGM 258176
S. lyrifer	RIN1	RGM 535210	RGM 535229	RGM 535320	RGM 535330
S. simplex	RIN1	RGM 535377	RGM 535402	RGM 535470	RGM 535498
T. hartenbergeri	ESC	Coll. Mein	coll. Mein	coll. Mein	coll. Mein
T. hartenbergeri	NO2	RGM 195545	RGM 195546		RGM 195547
V. autolensis	Quel			coll. Mein	
V. autolensis	STC		coll. Mein		coll. Mein
V. duplex	HRM1	Coll. Mein		coll. Mein	coll. Mein

Table 3. Locality codes.

Locality code	Locality name
AGT2D	Aguatón 2D
ALI1	Aliveri 1
ARM7	Armantes 7
BAL2	Balaruc 2
BAUZA	San Bauza
BEZ	Bézian
BIA1	Biancone 1
BN2	Bañón 2
BOU1	Bouzigues 1
CET	Cetina de Aragón
COD	Coderet
ESC	Escobosa
HAU	Hautimagne
HB	Hoogbutsel
HEIM	Heimersheim
HRM1	Harami 1
ITD	Itardies
KAM	Kamyk
KOC	Kocayarma
LAU	Laugnac
LGM	La Grive M
MIR1	Mirambueno 1
MIR4C	Mirambueno 4C
MIR4D	Mirambueno 4D
MLB1D	Montalbán 1D
MLB3Y	Montalbán 3Y
MLB8	Montalbán 8
NAV	Navarrete
NO2	Nombrevilla 2
OCE2C	Bco. de Oceca 2C
OLA4A	Olalla 4A
POV	Povoa de Santarem
RA1	Ramblar 1
RIN1	Rinascita 1
ROBIAC	Robiac
SG	San Giovannino
SMC	St.-Martin-de-Castillon
SS	Sansan
STC	Santa Cilia
TRK	Tourkobounia
UMB1B	Fuente Umbría 1B
VIV	Vivel del Río
WW	Wintershof-W

the distance between **x** and **y**, **h** (height) is the maximum depth of the concavity, and **S** is the surface of the area enclosed by **b** and the occlusal profile. The lines **b1** and **b2** are the portions of **b** defined by its intersection with **h**. The drawings have been rescaled, so that **w** = 10 in all cases; a test has shown that rescaling to **b** makes no difference in the results.

Best-Fitting Circle

The occlusal concavity of the profile of Figure 2 is a polygon, consisting of between 15 and 20 vertices connected by straight lines. To automate the process of finding the circle that best fits the concavity, circles were first constructed through all combinations of three vertices of the occlusal concavity, and the radius and center of each circle were calculated. Those circles with a center higher than the occlusal profile were discarded, because they correspond to convex parts of the profile; the distribution of the radii of all remaining circles was calculated, and the circles with extremely high or low values were discarded, too. Discarding 5% of the circles on each side of the distribution turned out to be a suitable procedure. Then a circle was drawn with its center at the mean of all circle centers, and a radius **r** corresponding to the mean of the radii. The radius of this circle was considered to be a first approximation of the circle that best fits the original curve. In the next step, the center of this circle was connected to all vertices, and the sum of the absolute values of the deviations **d-r** was calculated as **dev=** Σ **|dist-r|**, where **dist** is the distance from the circle center to the vertex. Then the circle was shrunk and wobbled through several thousand iterations to find the radius and the position of the circle that gave the lowest value for **dev**, and the radius **r** of that circle was then used as a measure of concavity. In the tables where **dev** is

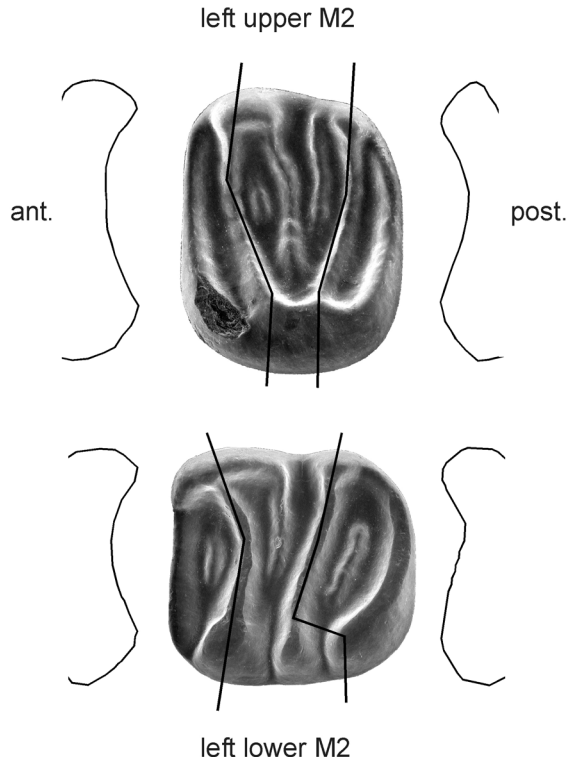

Figure 1. Location of the profiles in the occlusal surface.

listed, it is divided by the number of vertices **v** to standardize for **v**.

Several commercial computer programs permit drawing circles on bitmaps, and changing the position and radius of these circles. Our program makes this process much easier and maximizes precision, but results obtained through a program like Corel Draw are perfectly compatible, as we have tested by manually creating the circles and comparing them with the automatically obtained results. The difference of the radius of the programmatically calculated circle, and the one constructed manually in our tests, did not exceed 5%.

THE CONCAVITY PARAMETERS

Surface (S)

The surface (**S**) divided by **b** is certainly a good measure of convexity. It does not discriminate, however, between a triangular shape and a saucer shape. To eliminate scale differences, **S** is divided by **b**.

Height of the Profile (h)

The height (**h**) divided by **b** is another measure of convexity; it has the same inability to discriminate between triangular and saucer shapes as does **S**.

Best-Fitting Circle

The best-fitting circle, as defined previously, seems to be one of the best parameters to describe convexity. Of course the curve is not really part of a circle; maybe an ellipse would be a better approximation, but since the surface **S** is only a small part of the circle, another geometrical curve would only give the illusion of additional precision that is far beyond the accuracy of drawing the curve.

The convexity index C may be defined as the curvature of the circle, 1/r, as a function of **b**, **w**, or **h**, e.g.: C(b2r) = b/2r, C(w2r) = w/2r, C(hr) = h/r.

C(b2r) is infinitely small for completely flat molars, and its maximum is 1, when the diameter of the circle is identical to the length of **b**. An alternative is C(w2r), also infinitely small for completely flat molars, but C(w2r) may be larger than 1, espe-

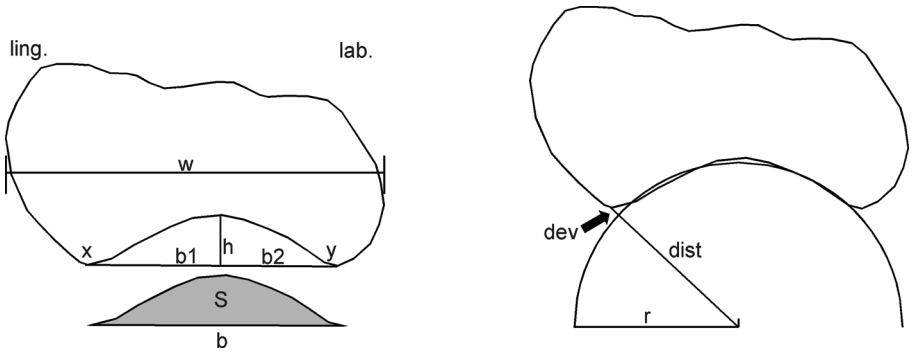

Figure 2. Parameters measured or calculated in the profile: **w** = the maximum width of the molar as seen in the profile, x and y are the limits of the occlusal concavity, **b** = the distance between x and y, **h** is the maximum depth of the concavity, **S** is the surface of the area enclosed by **b** and the occlusal profile; **b1** and **b2** are the portions of **b** defined by its intersection with **h**. **r** = the radius of the best-fitting circle, **dist** = the distance from the circle center to the occlusal profile, **dev** = **dist** - **r**.

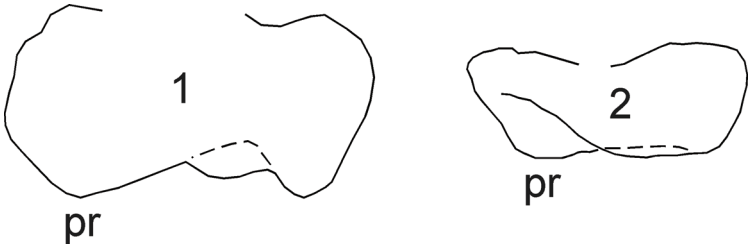

Figure 3. 3.1. *B. bruijni*, M_1 sin., MIR4C 1160; **3.2.** *G. majori*, M_1 sin., MIR4C 1028. Occlusal surface facing down, pr = protoconid.

cially in specimens where the top of the protocone lies far away from the lingual border of the tooth (in occlusal view), or, in other words, when the lingual slope of the protocone has an important horizontal component.

Another possibility is C(hr). In this case **h** is divided by **r**, instead of 2r, to force the maximum to be 1. As will be shown, C(hr) is probably the best concavity index.

In some cases the circle method gives an unsatisfactory result, e.g., when the profile is very asymmetric, when it is completely flat or even convex, or when the profile is formed by two almost straight lines, and approximation to a circle is poor.

BEST PARAMETERS

In order to decide which parameters are best for describing convexity we arranged the results for each of the eight profile classes in ascending order of the value of the first parameter (S). The sequence of the species thus obtained was compared with the sequences resulting from sorting the data in ascending order for each of the other parameters. The differences in rank order for each species were added, and the resulting sum used as an indicator of similarity, and this procedure was repeated, taking each one of the other parameters as the basis for comparison. The three parameters that gave the highest degree of similarity with all other parameters are for the lower molars: **h**, h/r, and b/2r; for the upper molars: h/r, b/2r, and h/b; and for the upper and lower molars together: h/r, b/2r, and h/b. Since h/r gives the highest degree of similarity between all profile classes, we decided to focus on that parameter. This does not mean that the other parameters are not useful. Our raw data are available to any reader interested in investigating the usefulness of the other parameters.

METHODOLOGICAL ISSUES

Profile Visibility

Our curves were drawn over protocone-paracone and protocone-metacone in the upper molars, and protoconid-metaconid and hypoconid-entoconid in the lowers. We had first considered using the anterior or posterior wall of the specimen, anteroloph(id) and posteroloph(id) respectively, but that profile was quite variable within a population.

The method we chose does not necessarily measure the complete profile of concavity because the actual profile along our transect may be partly obscured in the view from which the drawings were made: Figure 3 illustrates this showing a left M_1 of *B. bruijni* and *G. majori* in anterior view. The solid line shows the visible profile, and the dashed line shows the actual profile of the metalophid, which must be estimated because it is hidden behind the anterolophid. In principle the shape of the metalophid might be calculated by measuring the degree of inclination of the specimen at the point where anterolophid and metalophid coincide in vertical view, but such a calculation supposes a measure of accuracy that is not justified given the limitations of our method because of inherent errors that would be introduced by factors such as the vertical orientation of the specimen and parallax.

In some cases, we substituted a profile of the posterior border of the tooth (the posterolophid) because it was close to the profile we needed (e.g., the lower molars of *B. bravoi*). In other cases (*E. quercinus, B. bruijni*) the posterior profile was not visible in posterior view, but it could be drawn reliably in anterior view. In some species (*Glamys*) there was no connection between hypoconid and entoconid, and we constructed a composite curve of hypoconid, posterolophid, and entoconid for m1inf_post and m2inf_post.

Table 4. Effect of the distortion of the drawing in E-W orientation of the anterior profile. A + sign means an increased concavity index; in the posterior profile the effect is opposite.

Drawing	occ. surface facing	$M^{1,2}$ sin. ant.	$M^{1,2}$ dext. ant.
right-hand	N	+	-
right-hand	S	-	+
left-hand	N	-	+
left-hand	S	+	-

Parallax

In the following paragraphs we use North-South and East-West to describe the axes of a microscope field as if it were a compass. When we began drawing the curves, we oriented the specimens E-W, with the occlusal surface facing N. When we tested the reliability of curves by having various people draw the same specimen, we were confronted with a serious problem: in some cases there was no similarity whatsoever between a curve drawn by a right-handed person using the camera lucida on the right side of the microscope and a curve drawn by a left-handed person working on the opposite side. Exactly the same problem occurred when the same person drew the same specimen with the occlusal surface facing N then with it facing S.

We concluded that the inclined position of the microscope tube of a stereoscopic microscope tended to distort the curve. Drawing right-handed (camera lucida on the right side of the microscope), the right-hand part of the drawing is relatively shortened, and the left-hand part is stretched. Consequently, left-hand and right-hand molars that are exact mirror images of each other will yield completely different results. This distortion may not always happen, but it happens sufficiently often for this orientation to be rejected (see Table 4 and Figure 4). The parameters calculated from the three curves in Figure 4 are given in Table 5, where the different values for skewness illustrate the distortion through the displacement of the deepest point of the concavity.

A solution might be to use a non-stereoscopic microscope, but that is not a common instrument among students of fossil rodent teeth, and its relatively shallow depth of field would cause other problems.

We solved this problem by orienting the specimen N-S, with the occlusal surface facing to the side where the camera lucida is mounted. The depth of the concavity (**h**) is now oriented E-W, and if there is a distortion it affects the small value **h** and not the large value of the curve basis (**b**), and, if **h** is not a horizontal line, its inclination is always less than that of **b**. Furthermore, by facing the occlusal always to the side of the camera lucida, the distortion, if present, acts always in the same direction, regardless whether one draws left-handed or right-handed. It is evident that such a standardized orientation is fundamental for obtaining mutually comparable results.

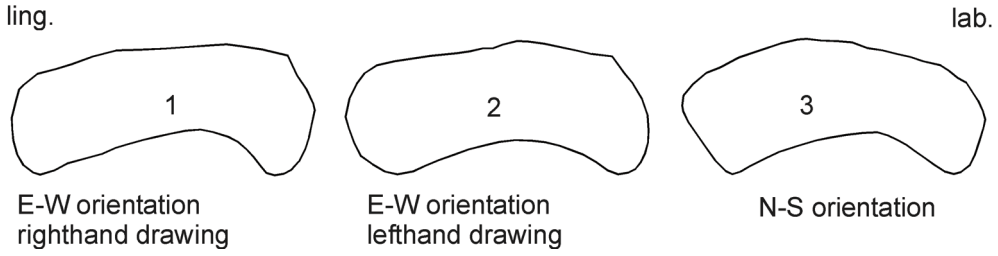

Figure 4. M^2 sin., anterior view, of *O. libanicus*, MLB8 1323. **4.1.** E-W orientation, drawn right-handed; **4.2.** E-W orientation, drawn left-handed; 4.3: N-S orientation.

Table 5. Parameters calculated for three different drawings of the same specimen (see Figure 4).

	S	w	B	h	S/b	h/b	r	h/r	b/2r	w/2r	skew	dev/v
E-W right	6.87	10.00	7.75	1.50	0.89	0.19	5.05	0.30	0.77	0.99	68.4	0.17
E-W left	4.98	10.00	7.28	1.12	0.68	0.15	4.16	0.27	0.88	1.20	53.0	0.16
N-S	6.05	10.00	7.30	1.38	0.83	0.19	4.43	0.31	0.82	1.13	65.4	0.11

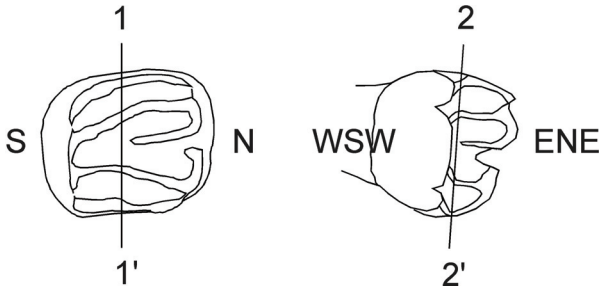

Figure 5. Orientation of M^2 sin.: 1-1') vertical line through deepest point of anterior and posterior profiles; 2-2') slightly inclined line, coinciding with the inclination of the microscope tube; both 1-1' and 2-2' through the deepest points of anterior and posterior profiles.

Vertical Orientation

Specimens were oriented vertically in a N-S orientation in such a way that the deepest point of the anterior profile and the deepest point of the posterior profile cover each other exactly. In the N-S plane these two points lie along a vertical line; in the E-W plane the line deviates slightly from the vertical, coinciding with the inclination of the microscope tube (see Figure 5). Figure 5.2 is almost perpendicular to Figure 5.1 and shows the same specimen with the view line 2-2' slightly inclined to coincide with the microscope tube.

Evidently the orientation of the specimen is important. This became clear while digitizing the eight anterior curves of *B. micio* published by Vianey-Liaud (1994; fig. 16) (= M-numbers in Table 6), and comparing them with our curves from specimens of the same species in the RGM collection. The results are given in Table 6. Among the M-numbers, three specimens are very concave, and five are much less so. Such a difference may well be due to the degree of wear, but the extremely high values of the three concave profiles could not be replicated by us using unworn specimens of the RGM collection. As a further experiment, we drew one specimen vertically, which yielded lower concavity values than the three very strongly concave profiles, and then drew the same specimen in an inclined position of about 65°, which yields much higher concavity values (see Table 6; values for h/r 0.24 versus 0.34). Apparently a false impression of concavity may be given when the orientation does not coincide strictly with the optical axis of the microscope tube.

This inclined orientation may well explain the high values for the three mentioned specimens. In fact, in the drawings by Vianey-Liaud (1994) one may observe the anteroloph drawn below the deepest point of the protoloph. In the RGM specimen in the (sub)vertical position, part of the profile of the protoloph has to be estimated because it is hidden by the anteroloph. So, probably, the specimens drawn by Vianey-Liaud were oriented obliquely to make the protoloph visible.

Table 6. Analysis of 10 anterior profiles of M^2 of *Butseloglis micio*. V' is the observed range of each parameter, expressed as percentage of the midpoint.

M^2 ant. *B. micio*	S	w	b	h	S/b	h/b	r	h/r	b/2r	w/2r	skew	dev/v
M1710	7.27	10.00	7.56	1.78	0.96	0.24	4.80	0.37	0.79	1.04	50.9	0.13
M1711	6.45	10.00	7.46	1.50	0.86	0.20	4.55	0.33	0.82	1.10	55.4	0.10
M1712	5.80	10.00	7.55	1.49	0.77	0.20	5.48	0.27	0.69	0.91	51.9	0.13
M1713	5.77	10.00	7.38	1.33	0.78	0.18	5.31	0.25	0.69	0.94	54.2	0.07
M1714	7.93	10.00	7.61	1.85	1.04	0.24	4.58	0.40	0.83	1.09	55.7	0.13
M1715	5.38	10.00	7.36	1.30	0.73	0.18	5.88	0.22	0.63	0.85	64.2	0.10
M1716	4.56	10.00	7.13	1.18	0.64	0.17	5.22	0.23	0.68	0.96	53.9	0.08
M1717	5.63	10.00	7.60	1.27	0.74	0.17	5.88	0.22	0.65	0.85	65.5	0.09
RGM 148878, 65º	6.14	10.00	6.97	1.44	0.88	0.21	4.23	0.34	0.82	1.18	46.1	0.06
RGM 148878, 90º	5.91	10.00	7.64	1.28	0.77	0.17	5.42	0.24	0.70	0.92	62.5	0.09
min.	4.56	10.00	6.97	1.18	0.64	0.17	4.23	0.22	0.63	0.85	46.10	0.06
mean	6.08	10.00	7.43	1.44	0.82	0.20	5.14	0.29	0.73	0.98	56.03	0.10
max.	7.93	10.00	7.64	1.85	1.04	0.24	5.88	0.40	0.83	1.18	65.50	0.13
sigma	0.95		0.22	0.22	0.12	0.03	0.57	0.07	0.08	0.11	6.22	0.03
midpoint	6.25		7.31	1.52	0.84	0.21	5.06	0.31	0.73	1.02	55.80	0.10
V'	54.0		9.2	44.2	47.6	34.1	32.6	58.1	27.4	32.5	34.8	73.7

Table 7. Statistical results for the anterior profile of M^2 of *O. libanicus*, MLB8 1323, drawn 15 times. V' is the range of each of the parameters as percentage of the midpoint.

	Surf	w	B	h	S/b	h/b	r	h/r	b/2r	w/2r	skew	dev/v
L-1	5.80	10.00	7.32	1.37	0.79	0.19	4.31	0.32	0.85	1.16	60.6	0.11
L-2	7.14	10.00	7.49	1.56	0.95	0.21	4.06	0.38	0.92	1.23	59.3	0.11
L-3	7.43	10.00	7.77	1.57	0.96	0.20	5.31	0.30	0.73	0.94	62.4	0.10
L-4	6.84	10.00	7.40	1.57	0.92	0.21	4.17	0.38	0.89	1.20	53.5	0.12
L-5	6.54	10.00	7.53	1.45	0.87	0.19	4.24	0.34	0.89	1.18	57.7	0.10
L-6	7.24	10.00	7.50	1.55	0.97	0.21	4.19	0.37	0.90	1.19	51.7	0.09
L-7	7.59	10.00	7.63	1.60	0.99	0.21	4.27	0.37	0.89	1.17	56.4	0.11
M-1	6.14	10.00	7.26	1.39	0.85	0.19	4.76	0.29	0.76	1.05	65.3	0.09
M-2	6.72	10.00	7.54	1.46	0.89	0.19	5.12	0.29	0.74	0.98	65.2	0.12
M-3	5.66	10.00	7.55	1.37	0.75	0.18	4.78	0.29	0.79	1.05	62.9	0.14
M-4	5.97	10.00	7.20	1.37	0.83	0.19	4.49	0.31	0.80	1.11	52.3	0.07
M-5	5.47	10.00	7.34	1.39	0.74	0.19	4.32	0.32	0.85	1.16	58.3	0.14
M-6	6.39	10.00	7.48	1.43	0.85	0.19	4.21	0.34	0.89	1.19	51.7	0.12
M-7	6.77	10.00	7.90	1.55	0.86	0.20	4.66	0.33	0.85	1.07	66.9	0.15
M-8	5.56	10.00	7.35	1.41	0.76	0.19	4.34	0.33	0.85	1.15	57.0	0.13
min.	5.47	10.00	7.20	1.37	0.74	0.18	4.06	0.29	0.73	0.94	51.70	0.07
mean	6.48	10.00	7.48	1.47	0.87	0.20	4.48	0.33	0.84	1.12	58.75	0.11
max.	7.59	10.00	7.90	1.60	0.99	0.21	5.31	0.38	0.92	1.23	66.90	0.15
sigma	0.70		0.19	0.09	0.08	0.01	0.37	0.03	0.06	0.09	5.10	0.02
midpoint	6.53		7.55	1.49	0.87	0.20	4.69	0.34	0.83	1.09	59.30	0.11
V'	32.5		9.3	15.5	28.9	15.4	26.7	26.9	23.0	26.7	25.6	72.7

Alternative Orientation

The problems of parallax distortion and visibility are inherent to the kind of microscope used. We considered orienting the specimens horizontally and using a microscope that allows vertical measurements. However, we were looking for a method that would be applicable for any researcher using the normally available stereoscopic microscope. A method using a confocal microscope, for example, would not be available to students who don't have access to such a special instrument. It cannot be denied, however, that the precision of a more expensive alternative would better control the problem of parallax than the method we present here.

Reliability and Repeatability

The orientation of the specimens inevitably implies a certain amount of error; therefore, a specimen of M^2 of *O. libanicus* from MLB8 was drawn several times by various people, each time after moving and reorienting the specimen. The results are given in Table 7, and give a good idea of the reliability of the method. The last row of the table gives the variation of each parameter as a percentage of the midpoint of the range. The error of orienting and drawing the specimen causes a variation of less then 15% on either side of the midpoint. The profiles of *M. misonnei*, drawn by Vianey-Liaud (1994), were analyzed and compared with the profiles of several specimens from the RGM collection drawn by the present authors. The results are quite comparable.

As a further test, the anterior profiles of eight specimens of M^2 of *B. itardiensis* from OLA4A were drawn and vectorized, in order to estimate the variation within a population. Table 8 represents the values obtained for each specimen and the mean and standard deviation of the various parameters.

We visually inspected additional specimens to determine whether our samples were adequate to characterize the typical concavity within a species. A total of 26 M^1 of *O. libanicus* from MLB8 were inspected without drawing them; 12 specimens were unworn and showed no obvious differences in concavity; among the remaining 14 specimens not a single one made us suspect an appreciably different degree of concavity.

Table 8. Variability of concavity parameters in the population of *B. itardiensis* from OLA4A.

	S	w	b	h	S/b	h/b	r	h/r	b/2r	w/2r	skew	dev/v
OLA4A 1063	4.74	10.00	6.72	1.24	0.70	0.18	4.92	0.25	0.68	1.02	59.6	0.09
OLA4A 1064	5.02	10.00	7.08	1.23	0.71	0.17	5.28	0.23	0.67	0.95	53.6	0.08
OLA4A 1065	5.07	10.00	7.17	1.23	0.71	0.17	5.29	0.23	0.68	0.95	55.7	0.09
OLA4A 1067	4.41	10.00	7.13	1.11	0.62	0.16	5.76	0.19	0.62	0.87	62.5	0.10
OLA4A 1070	5.85	10.00	7.48	1.26	0.78	0.17	5.57	0.23	0.67	0.90	57.3	0.04
RGM 386742	5.41	10.00	7.51	1.26	0.72	0.17	5.56	0.23	0.67	0.90	56.2	0.09
RGM 386746	4.52	10.00	7.34	1.15	0.62	0.16	5.81	0.20	0.63	0.86	59.3	0.09
RGM 386748	3.91	10.00	6.53	1.05	0.60	0.16	4.80	0.22	0.68	1.04	52.6	0.07
Min.	3.91	10.00	6.53	1.05	0.60	0.16	4.80	0.19	0.62	0.86	52.60	0.04
mean	4.87	10.00	7.12	1.19	0.68	0.17	5.37	0.22	0.66	0.94	57.10	0.08
max.	5.85	10.00	7.51	1.26	0.78	0.18	5.81	0.25	0.68	1.04	62.50	0.10
sigma	0.61		0.35	0.08	0.06	0.01	0.37	0.02	0.02	0.07	3.29	0.02

In order to test how well the circle coincides with the profile, the value of **dev** as defined in the Methods section, was divided by the number of vertices (**v**) that constitute the polygon. The deviation from the circle is on average slightly higher in the lower molars than in the upper ones (0.15 vs. 0.10), but the difference is not significant at a 5% confidence limit.

Also, for each profile a T-test was executed on the deviations from the circle. Among 510 profiles only 18 deviate significantly from a circle (at a 5% confidence level). These 18 profiles were equally distributed among lower and upper molars and among weakly and strongly concave profiles.

Though this method makes it possible for the first time to quantify concavity objectively, we note that orientation of the specimens is inevitably a subjective factor that may have considerable influence on the results. A partial solution to the problem of orientation would be to draw each specimen several times, and use the mean values calculated from these drawings.

Degree of Wear

Crown wear obviously influences observed concavity. Whenever possible we used unworn or minimally worn specimens, but such ideal specimens are not always available. Significantly worn specimens were always discarded, but in intermediate cases we found that it was possible to plausibly reconstruct the missing part of the worn cusps.

Normally wear affects the delimiting cusps first, and one may expect a gradually decreasing concavity from unworn to very worn specimens. The case of *B. concavidens* seems to indicate that there may be an increase in concavity during the first stages of wear (see the discussion of *Bransatoglis* in the Results section).

Skewness

Though not a measure of concavity, we also measured the skewness of the profiles, as defined by **b1** and **b2**; these values are identical in symmetric profile. In a very asymmetric curve **b1** and **b2** are substantially different. The skewness of the curve was measured as the percentage of **b** that is occupied by **b1**, or, in other words, 100 x **b1**/**b**.

Values around 50 indicate symmetric curves, low values mean that the deepest point of the concavity is lingual of the molar axis in the upper molars (labial of the axis in the lower molars); high values indicate the opposite.

When we started our investigation we decided to measure skewness, in order to find out if it played a role in concavity, because both skewness and concavity may play a role in different ways of occlusion. There is no apparent regularity in the distribution of the skewness. One would expect that there were a certain relation between the skewness value for the posterior profile of M1 and the anterior profile of M2, but that is not the case. Nor is there an evident pattern of distribution between the skewness of upper and lower profiles. Further study will have to show whether measuring skewness has some significance.

RESULTS

The values of the best parameters are listed in Table 9a (lower molars) and Table 9b (upper molars). Since h/r gave the highest degree of coincidence for all profile classes, we took that as the best index of concavity, which we call C(hr). The

Table 9. A. Statistics for the best parameters of the lower molars. Each subtable is sorted in ascending order of the mean of the first parameter. B. Statistics for the best parameters of the upper molars. Each subtable is sorted in ascending order of the mean of the first parameter. (Continued on next page.)

Part A: Lower Molars

m1inf_ant	h/r				b/2r				h			
	N	min.	mean	max.	N	min.	mean	max.	N	min.	mean	max.
Myomiminae	22	0.01	0.07	0.32	22	0.18	0.36	0.80	22	0.11	0.50	1.32
Microdyromys	7	0.03	0.09	0.15	7	0.27	0.42	0.55	7	0.30	0.68	0.97
Glirinae	3	0.03	0.12	0.30	3	0.25	0.42	0.71	3	0.44	0.85	1.62
Dryomyinae	7	0.05	0.14	0.27	7	0.31	0.51	0.72	7	0.55	0.85	1.28
Bransatoglis/Paraglis	3	0.10	0.14	0.19	3	0.47	0.55	0.63	3	0.76	0.91	1.02
Oligodyromys	5	0.14	0.22	0.36	5	0.52	0.64	0.82	5	0.87	1.16	1.72
Glamyinae	5	0.14	0.29	0.39	5	0.52	0.73	0.83	5	0.93	1.18	1.50
Gliravinae	6	0.03	0.31	0.53	6	0.31	0.72	0.95	6	0.24	1.15	1.58

m1inf_post	h/r				b/2r				h			
	N	min.	mean	max.	N	min.	mean	max.	N	min.	mean	max.
Myomiminae	22	0.00	0.09	0.19	22	0.00	0.41	0.67	22	0.00	0.61	0.95
Glirinae	3	0.05	0.13	0.26	3	0.34	0.49	0.76	3	0.46	0.86	1.45
Microdyromys	7	0.04	0.16	0.24	7	0.39	0.56	0.67	7	0.39	0.94	1.25
Bransatoglis/Paraglis	3	0.10	0.16	0.26	3	0.45	0.55	0.72	3	0.76	0.94	1.18
Gliravinae	6	0.04	0.21	0.35	6	0.34	0.64	0.80	6	0.43	1.09	1.55
Dryomyinae	7	0.07	0.23	0.40	7	0.38	0.65	0.84	7	0.57	1.12	1.55
Oligodyromys	5	0.11	0.23	0.32	5	0.48	0.67	0.80	5	0.76	1.18	1.51
Glamyinae	5	0.20	0.25	0.33	5	0.63	0.69	0.79	5	1.12	1.27	1.38

m2inf_ant	h/r				b/2r				h			
	N	min.	mean	max.	N	min.	mean	max.	N	min.	mean	max.
Myomiminae	22	0.01	0.09	0.23	22	0.16	0.43	0.64	22	0.05	0.66	1.30
Glirinae	4	0.04	0.11	0.29	4	0.33	0.46	0.75	4	0.39	0.76	1.53
Microdyromys	7	0.06	0.13	0.23	7	0.37	0.51	0.64	7	0.62	0.91	1.23
Dryomyinae	7	0.07	0.19	0.35	7	0.41	0.58	0.80	7	0.59	1.04	1.44
Bransatoglis/Paraglis	3	0.16	0.20	0.23	3	0.56	0.65	0.69	3	1.05	1.13	1.27
Gliravinae	6	0.08	0.22	0.52	6	0.44	0.63	0.94	6	0.54	1.02	1.75
Oligodyromys	6	0.16	0.24	0.30	6	0.54	0.67	0.73	6	0.95	1.19	1.35
Glamyinae	6	0.11	0.28	0.43	6	0.49	0.71	0.90	6	0.68	1.22	1.59

m2inf_post	h/r				b/2r				h			
	N	min.	mean	max.	N	min.	mean	max.	N	min.	mean	max.
Myomiminae	22	0.00	0.09	0.20	22	0.00	0.42	0.68	22	0.00	0.61	1.15
Glirinae	3	0.04	0.10	0.21	3	0.29	0.43	0.67	3	0.45	0.70	1.20
Microdyromys	7	0.05	0.13	0.35	7	0.34	0.50	0.82	7	0.54	0.86	1.62
Gliravinae	6	0.10	0.17	0.26	6	0.48	0.60	0.71	6	0.72	0.95	1.20
Oligodyromys	5	0.15	0.19	0.21	5	0.60	0.63	0.67	5	0.87	1.03	1.11
Dryomyinae	7	0.08	0.20	0.32	7	0.41	0.62	0.80	7	0.69	1.08	1.44
Glamyinae	6	0.14	0.23	0.29	6	0.57	0.66	0.75	6	0.83	1.16	1.44
Bransatoglis/Paraglis	3	0.13	0.23	0.38	3	0.53	0.67	0.87	3	0.81	1.22	1.73

Table 9 (continued).

Part B: Upper Molars

m1sup_ant		h/r				b/2r				h/b		
	N	min.	mean	max.	N	min.	mean	max.	N	min.	mean	max.
Glirinae	5	0.07	0.15	0.39	5	0.38	0.50	0.83	5	0.10	0.13	0.24
Myomiminae	22	0.06	0.16	0.25	22	0.37	0.56	0.68	22	0.09	0.14	0.18
Bransatoglis/Paraglis	3	0.20	0.21	0.21	3	0.64	0.65	0.66	3	0.16	0.16	0.17
Microdyromys	7	0.09	0.24	0.33	7	0.44	0.66	0.77	7	0.11	0.17	0.21
Dryomyinae	7	0.08	0.26	0.42	7	0.40	0.69	0.89	7	0.10	0.18	0.24
Oligodyromys	6	0.17	0.27	0.33	6	0.58	0.70	0.77	6	0.15	0.19	0.22
Gliravinae	6	0.19	0.30	0.40	6	0.61	0.74	0.85	6	0.15	0.20	0.24
Glamyinae	6	0.23	0.31	0.46	6	0.66	0.76	0.91	6	0.17	0.20	0.25

m1sup_post		h/r				b/2r				h/b		
	N	min.	mean	max.	N	min.	mean	max.	N	min.	mean	max.
Glirinae	4	0.08	0.14	0.30	4	0.41	0.50	0.75	4	0.10	0.13	0.20
Myomiminae	21	0.08	0.16	0.30	21	0.39	0.56	0.78	21	0.10	0.14	0.19
Bransatoglis/Paraglis	3	0.16	0.17	0.17	3	0.57	0.58	0.60	3	0.14	0.14	0.15
Dryomyinae	7	0.09	0.18	0.23	7	0.42	0.59	0.68	7	0.11	0.15	0.18
Microdyromys	7	0.11	0.19	0.23	7	0.48	0.63	0.69	7	0.11	0.15	0.18
Glamyinae	6	0.14	0.21	0.28	6	0.54	0.64	0.76	6	0.13	0.17	0.18
Oligodyromys	6	0.16	0.22	0.26	6	0.58	0.66	0.71	6	0.14	0.17	0.19
Gliravinae	6	0.13	0.24	0.37	6	0.51	0.66	0.84	6	0.13	0.17	0.22

m2sup_ant		h/r				b/2r				h/b		
	N	min.	mean	max.	N	min.	mean	max.	N	min.	mean	max.
Glirinae	7	0.06	0.12	0.19	7	0.36	0.48	0.60	7	0.09	0.12	0.16
Myomiminae	23	0.06	0.20	0.34	23	0.36	0.61	0.79	23	0.08	0.16	0.22
Microdyromys	10	0.15	0.22	0.27	10	0.56	0.65	0.73	10	0.14	0.17	0.19
Gliravinae	7	0.19	0.24	0.31	7	0.59	0.69	0.76	7	0.16	0.17	0.20
Dryomyinae	9	0.09	0.24	0.43	9	0.43	0.66	0.85	9	0.10	0.17	0.25
Oligodyromys	9	0.16	0.25	0.36	9	0.56	0.69	0.79	9	0.14	0.18	0.23
Bransatoglis/Paraglis	8	0.16	0.27	0.33	8	0.57	0.71	0.77	8	0.14	0.19	0.22
Glamyinae	6	0.21	0.28	0.34	6	0.64	0.72	0.80	6	0.16	0.19	0.22

m2sup_post		h/r				b/2r				h/b		
	N	min.	mean	max.	N	min.	mean	max.	N	min.	mean	max.
Glirinae	5	0.04	0.11	0.16	5	0.31	0.47	0.57	5	0.07	0.11	0.14
Myomiminae	23	0.03	0.14	0.26	23	0.24	0.52	0.73	23	0.06	0.13	0.18
Dryomyinae	8	0.05	0.15	0.33	8	0.31	0.52	0.78	8	0.08	0.13	0.21
Glamyinae	6	0.11	0.17	0.25	6	0.45	0.57	0.69	6	0.12	0.15	0.18
Gliravinae	7	0.11	0.18	0.33	7	0.49	0.58	0.78	7	0.11	0.15	0.21
Microdyromys	10	0.10	0.18	0.24	10	0.44	0.59	0.67	10	0.11	0.15	0.19
Oligodyromys	8	0.14	0.19	0.29	8	0.51	0.62	0.78	8	0.13	0.16	0.18
Bransatoglis/Paraglis	5	0.19	0.24	0.34	5	0.64	0.70	0.80	5	0.15	0.17	0.21

Table 10. Values of C(hr), sorted by group, genus, and species. Each line represents one specimen per element; when more than one specimen per element was measured, it occupies a separate line. (Continued on next three pages).

h/r		M_1		M_2		M^1		M^2	
group	species	ant	post	ant	post	ant	post	ant	post
Oligodyromys	*Oligodyromys attenuatus*	0.14	0.11	0.17	0.15	0.17	0.16	0.16	0.15
	Oligodyromys libanicus MLB3Y	0.19	0.24	0.28	0.20	0.33	0.20	0.28	0.21
	Oligodyromys libanicus MLB8	0.14	0.20	0.29	0.21	0.30	0.24	0.26	0.25
	Oligodyromys parvus	0.27	0.26	0.30	0.19	0.20	0.20	0.21	0.17
	Oligodyromys parvus (2)					0.30	0.25		
	Oligodyromys planus HB							0.17	0.14
	Oligodyromys planus HB (2)							0.25	0.14
	Oligodyromys planus HEIM			0.16				0.26	0.20
	Oligodyromys planus SMC							0.28	
	Oligodyromys sjeni	0.36	0.32	0.24	0.18	0.32	0.26	0.36	0.29
Bransatoglis *Paraglis*	*Bransatoglis cadeoti*			0.21	0.13	0.20	0.16	0.24	0.19
	Bransatoglis concavidens	0.10	0.12	0.23	0.38			0.32	0.34
	Bransatoglis concavidens (2)							0.24	
	Paraglis astaracensis	0.14	0.10	0.16	0.18	0.21	0.17	0.16	0.22
	Paraglis astaracensis POV					0.21	0.17		
	Paraglis fugax							0.33	0.23
	Paraglis fugax (2)							0.28	
	Paraglis fugax (3)							0.32	
	Paraglis infralactorensis	0.19	0.26					0.27	0.24
Microdyromys	*Microdyromys complicatus*	0.11	0.20	0.10	0.06	0.23	0.23	0.15	0.24
	Microdyromys complicatus ARM7	0.06	0.15	0.14	0.14			0.22	0.11
	Microdyromys legidensis	0.12	0.22	0.09	0.09	0.09	0.13	0.25	0.19
	Microdyromys misonnei HB	0.15	0.11	0.23	0.35	0.29	0.22	0.27	0.19
	Microdyromys misonnei HB (2)							0.19	0.10
	Microdyromys misonnei MLB1D	0.10	0.24	0.16	0.15	0.28	0.23	0.20	0.19
	Microdyromys misonnei MLB1D (2)					0.17	0.22	0.17	0.20
	Microdyromys praemurinus MIR1	0.03	0.04	0.06	0.05	0.26	0.11	0.22	0.17
	Microdyromys praemurinus VIV	0.06	0.13	0.14	0.08	0.33	0.22	0.26	0.17
	Microdyromys praemurinus VIV (2)							0.27	0.19

remaining discussion concentrates on that parameter. The values obtained for h/r for each specimen are listed in Table 10.

C(hr) gave a wide range for m2sup_ant, from 0.09 for *M. praemurinus* to 0.33 for *G. bravoi*. Values for m2sup_post on the other hand, ranged from 0.07 for *O. attenuatus* to 0.21 for *O. libanicus*, and in many cases the value for m2sup_post was only little more than half the value for m2sup_ant. This was due to the fact that in many species the metacone was considerably lower than the paracone.

When paracone and metacone were similar in height, the two indices were fairly close. For example in *O. attenuatus*, m1sup_ant and m1sup_post had almost identical values, paracone and metacone were equally high, as were m2sup_ant and m2sup_post. On the other hand, in the specimens of *M. misonnei* from HB in both M^1 and M^2 the metacone was much lower than the paracone and the posterior branch of the trigone-V was sometimes shorter than the anterior branch, which resulted in higher concavity values for the anterior profiles.

In Figures 6.1 and 6.2 the horizontal bars give the range of C(h/r) for each group. The position of each individual specimen is indicated by a + sign within each range bar, in some cases slightly offset

Table 10 (continued).

Dryomyinae	*Dryomys apulus*			0.12	0.16	0.19	0.23	0.20	0.18
	Dryomys nitedula					0.25	0.09	0.30	0.11
	Eliomys intermedius	0.26	0.36	0.16	0.32	0.42	0.23	0.43	0.33
	Eliomys quercinus	0.27	0.22	0.35	0.32	0.40	0.22	0.33	0.20
	Eliomys truci	0.08	0.12	0.11	0.16			0.09	0.05
	Hypnomys morpheus	0.12	0.40	0.34	0.24	0.36	0.21	0.27	
	Maltamys wiedincitensis	0.05	0.21	0.07	0.08			0.11	0.06
	Paraglirulus agelakisi	0.09	0.07	0.16	0.12	0.15	0.17	0.19	0.16
	Paraglirulus conjunctus	0.10	0.24			0.08	0.11	0.21	0.11
Glamyinae	*Glamys devoogdi*	0.35	0.28	0.17	0.20	0.23	0.14	0.21	0.11
	Glamys olallensis	0.39	0.24	0.36	0.29	0.36	0.22	0.34	0.25
	Glamys priscus	0.14	0.33	0.40	0.26	0.27	0.21	0.27	0.14
	Glamys robiacensis	0.22	0.20	0.43	0.26	0.26	0.28	0.32	0.19
	Glamys umbriae	0.33	0.22	0.22	0.22	0.25	0.17	0.23	0.18
	Glamys sp.			0.11	0.14	0.46	0.25	0.31	0.15
Gliravinae	*Butseloglis bravoi*	0.43	0.35	0.20	0.14	0.40	0.37	0.29	0.17
	Butseloglis bruijni	0.37	0.28	0.11	0.14	0.19	0.14	0.19	0.19
	Butseloglis bruijni (2)							0.19	0.12
	Butseloglis itardiensis	0.53	0.18	0.52	0.17	0.29	0.29	0.23	0.15
	Butseloglis micio	0.29	0.20	0.33	0.20	0.34	0.31	0.25	0.17
	Butseloglis montisalbani	0.18	0.20	0.10	0.26	0.34	0.17	0.31	0.33
	Gliravus majori	0.03	0.04	0.08	0.10	0.21	0.13	0.24	0.11
Glirinae	*Glirudinus antiquus*			0.07		0.08		0.10	
	Glirudinus antiquus Figure u3							0.19	
	Glirudinus glirulus			0.04	0.04	0.13	0.08	0.06	0.04
	Glis guerbuezi	0.30	0.26	0.29	0.21	0.39	0.30	0.19	0.16
	Glirudinus modestus BN2	0.04	0.05	0.05	0.04	0.07	0.09	0.10	0.13
	Glirudinus modestus BOU1					0.08	0.08	0.10	0.11
	Glis sackdillingensis	0.03	0.07					0.11	0.11

to enhance the visibility of all the points. The black/white bar on top of m2sup_ant represents twice the standard deviation of the multiple drawings of *O. libanicus*, taken from Table 7. That bar gives an idea of the reliability of each of the individual values as represented by the + signs.

The maximum values range between 0.32 (m2inf_post Dryomyinae) and 0.53 (m1inf_ant Gliravinae); for each one of the eight profile classes this maximum value is divided by three, in order to define the limits of weakly concave, moderately concave, and strongly concave. The dashed vertical lines represent these limits. Their values are listed in Table 11.

In order to compare the concavity of upper and lower molars, for each species the mean of the values of C(hr) of M_1 and M_2 was compared to the mean of C(hr) of M^1 and M^2 (see Figure 7). The oblique line denotes equal concavity in upper and lower molars; to the left of that line the upper molars are more concave than the lower ones.

DISCUSSION

Oligodyromys (group 1)

The small Eocene and Lower Oligocene species of Bransatoglirinae have moderately to strongly concave upper and lower molars. As the name indicates, *Oligodyromys planus* is supposed to have relatively flat molars but it possesses moderately concave molars. Within this group *O. sjeni* possesses the strongest concave molars, and *O. attenuatus* possesses the least concave ones. The

Table 10 (continued). Values of C(hr), sorted by group, genus, and species.

h/r		M_1		M_2		M^1		M^2	
group	species	ant	post	ant	post	ant	post	ant	post
	Armantomys aragonensis							0.20	0.06
	Altomiramys daamsi	0.02	0.03	0.01	0.02	0.13	0.10	0.17	0.05
	Armantomys parsani	0.02	0.04			0.11	0.10	0.17	0.11
	Armantomys tricristatus	0.03	0.00	0.07	0.00			0.06	0.03
	Dryomimus eliomyoides	0.13	0.19	0.11	0.19	0.06	0.19	0.20	0.20
	Myomimus dehmi	0.32	0.13	0.18	0.06	0.12	0.19	0.34	0.19
	Nievella mayri			0.23	0.17	0.19	0.12		
	Pseudodryomys aguirrei	0.05	0.16	0.07	0.07	0.16	0.08	0.19	0.09
	Prodryomys brailloni	0.10	0.05	0.12	0.11	0.11	0.13	0.10	0.07
	Praearmantomys crusafonti	0.03	0.11	0.09	0.13			0.18	0.17
	Prodryomys gregarius	0.03	0.16	0.08	0.05	0.19	0.24	0.20	0.22
Myominae	*Pseudodryomys ibericus*	0.04	0.05	0.06	0.04	0.23	0.21	0.12	0.08
	Peridyromys jaegeri					0.18	0.19		
	Peridyromys murinus	0.10	0.10	0.09	0.05	0.25	0.30	0.33	0.19
	Peridyromys murinus RA1	0.02	0.07	0.06	0.20	0.20	0.21		
	Pseudodryomys simplicidens	0.01	0.03	0.05	0.03	0.13	0.09	0.29	0.11
	Stertomys aff. *daamsi*	0.03	0.09	0.12	0.17	0.23	0.11	0.24	0.16
	Stertomys daamsi	0.03	0.06	0.03	0.07	0.14	0.10	0.07	0.12
	Stertomys daunius	0.09	0.06	0.08	0.06	0.12	0.19	0.10	0.19
	Stertomys laticrestatus	0.12	0.12	0.11	0.07	0.18		0.17	0.15
	Stertomys lyrifer	0.05	0.10	0.12	0.08	0.22	0.15	0.26	0.20
	Stertomys simplex	0.06	0.09	0.04	0.01	0.18	0.15	0.20	0.12
	Tempestia hartenbergeri	0.06	0.08	0.11	0.03			0.29	0.26
	Tempestia hartenbergeri ESC	0.05	0.10	0.14	0.20	0.13	0.17	0.22	0.16
	Vasseuromys autolensis			0.10	0.19	0.15	0.18	0.26	0.12
	Vasseuromys duplex	0.05	0.08			0.12	0.11	0.23	0.14

lower molars are less concave than the upper ones.

Bransatoglis/Paraglis (group 2)

These large species from the Upper Oligocene and Miocene have the same range of concavity as the previous group, in general, moderately concave. The M^2 of *P. fugax* is strongly concave, and data for the other elements are not available.

The M^2 of *B. concavidens* is strongly concave, but not much more than *O. planus*; the value obtained may be exaggerated, because wear seems to affect more the center of the tooth than the labial and lingual border. Its M_1 is only weakly concave, and its M_2 is moderately concave (the very high value for m2inf_post of *B. concavidens* is misleading, because the profile had to be drawn over the posterolophid).

Microdyromys (group 3)

This group may be defined as weakly to moderately concave, clearly less than the previous groups. The posterior profile of M^2 is an exception in being strongly concave in various cases. The lower molars are clearly less concave than in the previous two groups, and less concave than the upper ones. Like in the case of *B. concavidens*, m2inf_post is strongly concave in one case (*M. misonnei* from HB), due to the fact that the posterolophid was drawn instead of the line over hypoconid-entoconid.

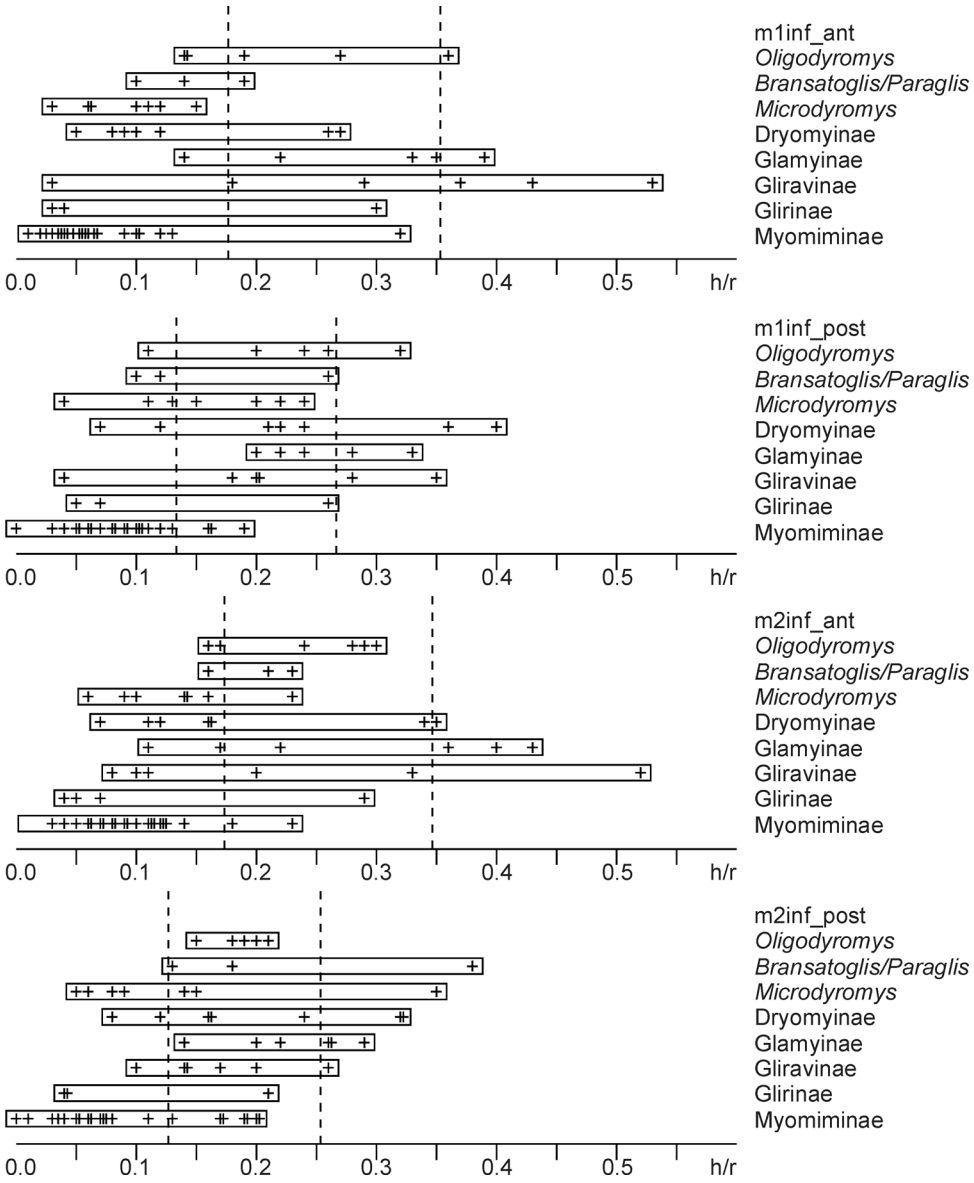

Figure 6. 6.1. Distribution of C(hr) in the lower molars.(Continued on next page.)

Dryomyinae (group 4)

Concavity has a very wide range, from weakly to strongly concave, both in the group as a whole and intragenerically: *Eliomys intermedius* is among the most concave Gliridae, whereas *E. truci* has molars that are only weakly concave. Upper and lower molars have about the same degree of concavity.

Glamyinae (group 5)

Glamyinae have moderately to strongly concave molars with relatively little variation. Generally the lower molars are more concave than the upper ones.

Gliravinae (group 6)

The upper molars are moderately to strongly concave. In the lower molars, the profiles are almost flat in *Gliravus majori*, and very strongly concave in *Butseloglis*, especially *B. itardiensis*. This indicates a completely different mechanism of occlusion and mastication between both species. It is not clear whether this may have taxonomic consequences.

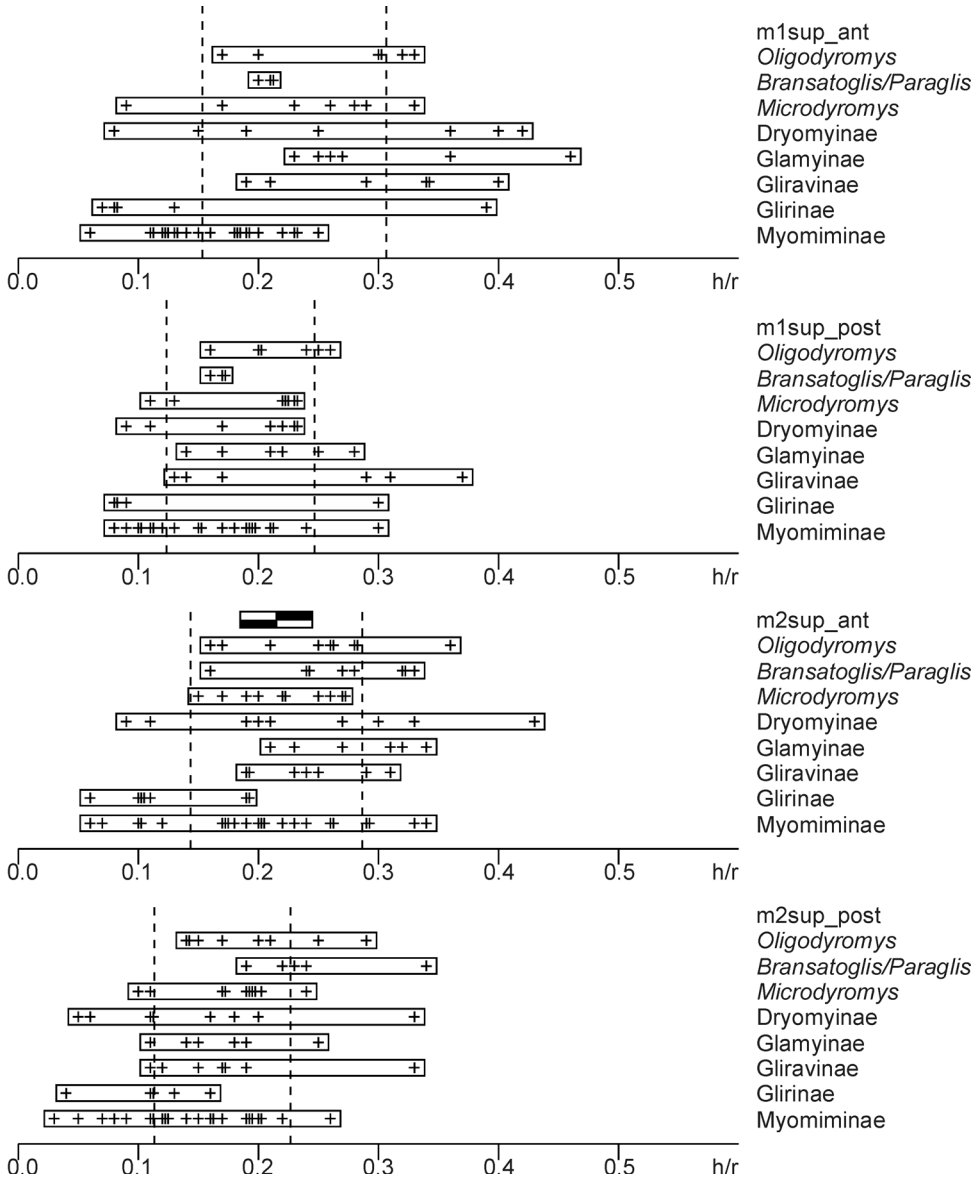

Figure 6. (Continued from previous page.) **6.2.** Distribution of C(hr) in the upper molars.

Table 11. Limits of weakly, moderately, and strongly concave for the eight profile classes.

Concavity	Weak	Moderate	Strong
m1inf_ant	0 - 0.18	0.18 - 0.35	> 0.35
m1inf_post	0 - 0.13	0.13 - 0.27	> 0.27
m2inf_ant	0 - 0.17	0.17 - 0.35	> 0.35
m2inf_post	0 - 0.13	0.13 - 0.25	> 0.25
m1sup_ant	0 - 0.15	0.15 - 0.31	> 0.31
m1sup_post	0 - 0.12	0.12 - 0.25	> 0.25
m2sup_ant	0 - 0.14	0.14 - 0.29	> 0.29
m2sup_post	0 - 0.11	0.11 - 0.23	> 0.23

Glirinae (group 7)

Though our data are scarce, molars of Glirinae may be defined as only weakly concave. However, *Glis guerbuezi* has much stronger concave molars, to such an extent that one should seriously doubt, whether its classification as a Glirinae is correct.

Vianey-Liaud (2004) figured two anterior profiles of M^2 of *Glirudinus antiquus*. One of these is weakly concave (ITD 316, Figure 2j3), the other one is moderately concave (ITD 331, Figure 2u3); the difference between the two is large, and one might consider whether ITD 331 is a *Microdyromys*; the size distribution of *G. antiquus* partly

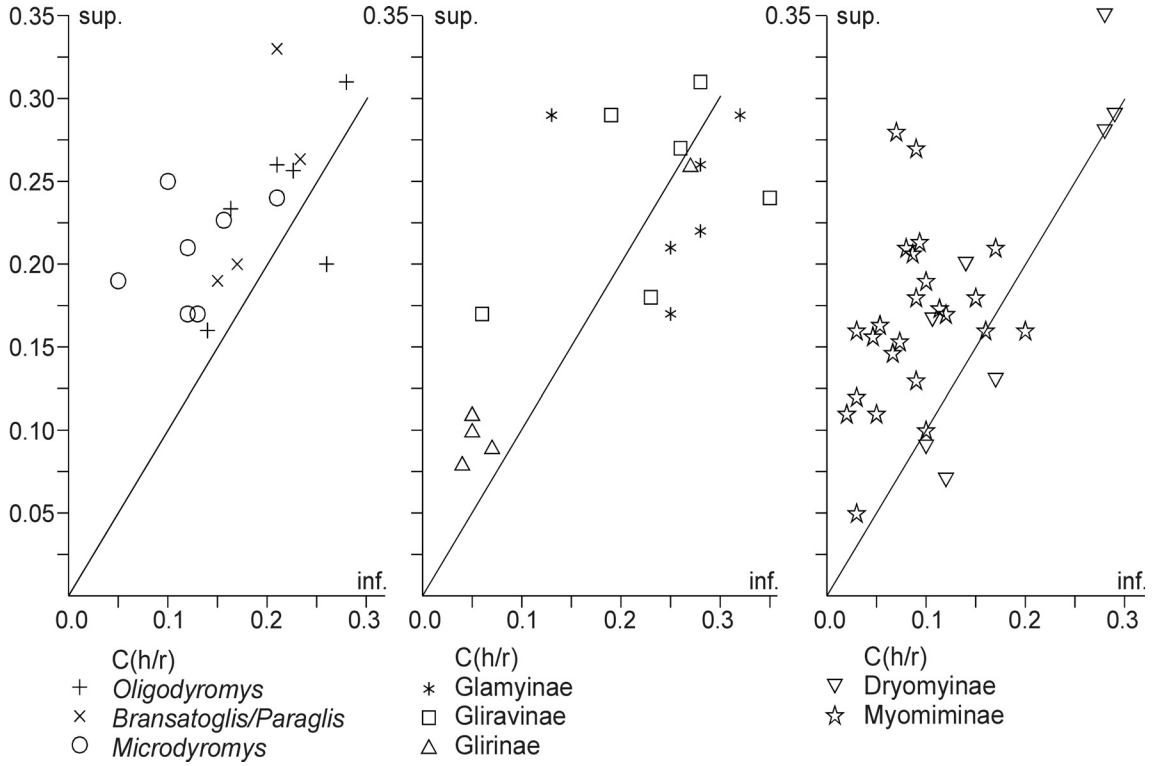

Figure 7. Comparison of the mean of C(hr) of $M^{1,2}$ with that of $M_{1,2}$.

overlaps that of the contemporaneous *M. misonnei* from MLB1D.

Myomiminae (group 8)

Myomiminae have molars that are generally weakly to moderately concave, but with a very wide range of variation, and a few cases even possess strongly concave upper molars. The lower molars are nearly always less concave than the upper ones.

Concavity through Time

In Table 12 the eight glirid groups are characterized by the concavity of their molars. Concavity does not give an absolute distinction between groups, but it does serve to characterize the groups.

Weakly concave molars are a derived character, not observed in Glamyinae and *Oligodyromys*. Figure 8 shows that these two groups are the oldest Gliridae, together with Gliravinae, and that they are restricted to the Late Eocene and Early Oligocene. Weak concavity appears for the first time in the Gliravinae (*Gliravus majori*) in ELMA MP 26, and in all the other groups later in the Late Oligocene, except in Dryomyinae, which are only known from the Miocene onwards. Glirinae and Myomiminae appear in MP28, and their first representatives already show this feature. These groups are derived from the Gliravinae (Daams and de Bruijn 1995), and they may have inherited this feature from that group. *Microdyromys* develops it at the same time, or maybe somewhat earlier (MP 27), independently from the other groups. *Bransatoglis* develops it in MP30, apparently independent of the other cases too. There exists a doubtful record of this genus in MP 25 (see Freudenthal and Martín Suárez, in press), which might link *Bransatoglis concavidens* to *Oligodyromys*.

Moderate concavity occurs in all groups. Strong concavity, considered to be the original situation, is absent or doubtful in Glirinae and Myominae, which appear to be the most advanced groups.

Oligodyromys planus, weakly concave according to the original description, must be characterized as moderately concave. *Bransatoglis concavidens* is strongly concave indeed, but only in its M^2.

An objective definition of concavity may have taxonomic consequences at supraspecific level, but it is too early for that. In spite of the large amount of data, 500 profiles distributed over 60 species, the vast majority of the species is represented by one specimen per dental element only.

Table 12. Characterization of the concavity of the eight glirid groups. (x) represents rare or doubtful cases.

	Lower Molars			Upper Molars		
	Weak	**Moderate**	**Strong**	**Weak**	**Moderate**	**Strong**
Oligodyromys		x	(x)		x	X
Bransatoglis/Paraglis	x	x	(x)		x	X
Microdyromys	x	x	(x)	x	x	(x)
Dryomyinae	x	x	x	x	x	X
Glamyinae		x	x		x	X
Gliravinae	x	x	x		x	X
Glirinae	x	(x)		x	x	(x)
Myomiminae	x	x		x	x	(x)

An unknown factor is the relation between concavity and occlusion. In some cases strongly concave upper molars come with strongly concave lower ones, but in other cases they combine with almost flat lower molars. Their occlusion and mastication process must be quite different.

Analysis of the population of *Butseloglis itardiensis* from OLA4A shows that the variation within a sample is reasonable, but analysis of 15 profiles of the same specimen of *Oligodyromys libanicus* from MLB8 reveals a fairly large error, probably due to orientation of the specimen. It is advisable to draw each specimen several times and use the mean values obtained from these drawings. That will reduce the error considerably. Though the calculations are completely objective, the orientation of the specimen inevitably has a subjective factor that may have considerable influence on the results.

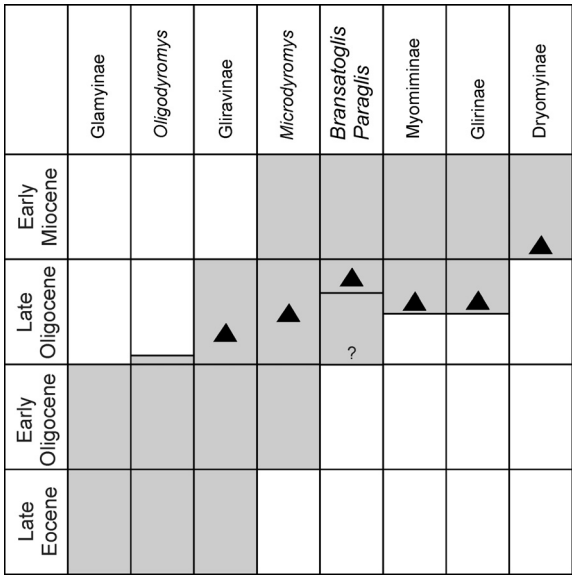

Figure 8. Stratigraphic distribution of the eight groups of Gliridae. The black triangles indicate the first appearance of weakly concave molars in each group.

CONCLUSIONS

Estimating concavity descriptively is subjective and may yield quite different assessments depending on the researcher. The method described in this paper gives fairly reliable, objective results. Processing a large number of profiles (over 500 in this paper) would have been almost impossible without computer programs especially written for this task. However, even though we automated the processing, others can reliably calculate comparable concavity parameters with a commercial program, like Corel Draw or Cadcam. We applied this method to glirid molars, but in principle it could be applied to any concave or convex surface with little modification.

Our quantitative indices of concavity may require taxonomic revision of glirids at the supraspecific level because our results were often at odds with the comparative assessment of concavity by previous workers in the field. But it is too early to make a more certain statement because our data for most species were based on only one specimen per dental element. Intraspecific variability in concavity is so far known in one case only.

The relation between concavity and occlusion requires further attention.

ACKNOWLEDGEMENTS

Thanks are due to Dr. M.T. Lamata (Granada) for discussing the mathematical basis of this paper. Dr. P. Mein (Lyon) gave us access to his collections. Dr. M. Hugueney (Lyon) provided us with several unpublished profile drawings. This study was executed in the framework of research group RNM 0190 of the 'Junta de Andalucia' and the

project Consolider Ingenio 2010, CSD 2006-00041. We wish to thank two anonymous referees who suggested many improvements of this paper.

REFERENCES

Adrover, R. 1978. Les Rongeurs et Lagomorphes (Mammalia) du Miocène inférieur continental de Navarrete del Río (province de Teruel, Espagne). *Documents du Laboratoire de Géologie de la Faculté des Sciences de Lyon*, 72:3-47.

Aguilar, J.P. 1974. Les Rongeurs du Miocène inférieur en Bas-Languedoc et les corrélations entre échelles stratigraphiques marine et continentale. *Géobios*, 7, 4:345-398.

Bahlo, E. 1975. Die Nagetierfauna von Heimersheim bei Alzey (Rheinhessen, Westdeutschland) aus dem Grenzbereich Mittel/Oberoligozän und ihre stratigrafische Stellung. *Abhandlungen Hessisches Landesamt für Bodenforschung*, 71:1-182.

Bate, D.M.A. 1918. On a new genus of extinct Muscardine Rodent from the Balearic Islands. *Proceedings of the Zoological Society London*:209-222.

Baudelot, S. 1970. Compléments à l'étude des micromammifères du gisement Miocène de Sansan (Gers). *Comptes Rendus sommaires Société Géologique de France*, 8:303-304.

Baudelot, S. and Collier, A. 1982. Les faunes de mammifères miocènes du Haut-Armagnac (Gers, France): Les Gliridés (Mammalia, Rodentia). *Géobios*, 15,5:705-727.

Bosma, A. and de Bruijn, H. 1979. Eocene and Oligocene Gliridae (Rodentia, Mammalia) from the Isle of Wight, England. Part 1. The *Gliravus priscus - Gliravus fordi* lineage. *Proceedings Koninklijke Nederlandse Akademie van Wetenschappen, B*, 82, 4:367-384.

Bulot, C. 1978. *Bransatoglis cadeoti* n. sp., un nouveau Gliridae (Rodentia, Mammalia) du Miocène de Bézian (Zone de la Romieu). *Géobios*, 11, 1:101-106.

Cuenca, G. 1985. Los roedores (Mammalia) del Mioceno inferior de Autol (Rioja). *Instituto de Estudios Riojanos, Logroño*, 1985, 2:1-96.

Daams, R. 1976. Miocene Rodents (Mammalia) from Cetina de Aragón (Prov. Zaragoza) and Buñol (Prov. Valencia), Spain. *Proceedings Koninklijke Nederlandse Akademie van Wetenschappen, B*, 79, 3:152-182.

Daams, R. 1981. The dental pattern of the dormice *Dryomys*, *Myomimus*, *Microdyromys* and *Peridyromys*. *Utrecht Micropaleontological Bulletins, Special Publication*, 3:1-115.

Daams, R. 1990. Hypsodont Myomiminae (Gliridae, Rodentia) from the Miocene and the Oligocene-Miocene boundary interval of Spain. *Scripta Geologica*, 95:1-63.

Daams, R. and de Bruijn, H. 1995. A classification of the Gliridae (Rodentia) on the basis of dental morphology. *Hystrix*, 6, 1-2:3-50.

Daams, R. and Freudenthal, M. 1985. *Stertomys laticrestatus*, a new glirid (dormice, Rodentia) from the insular fauna of Gargano (Prov. of Foggia, Italy). *Scripta Geologica*, 77:21-27.

de Bruijn, H. 1966a. Some new Miocene Gliridae (Rodentia, Mammalia) from the Calatayud Area (prov. Zaragoza, Spain). *Proceedings Koninklijke Nederlandse Academie van Wetenschappen, B,*, 69, 1:1-21.

de Bruijn, H. 1966b. On the Mammalian fauna of the Hipparion-Beds in the Calatayud-Teruel Basin (prov. Zaragoza, Spain). Part II. The Gliridae (Rodentia). *Proceedings Koninklijke Nederlandse Akademie van Wetenschappen, B*, 69:58-78.

de Bruijn, H. 1967. Gliridae, Sciuridae y Eomyidae (Rodentia, Mammalia) miocenos de Calatayud (provincia de Zaragoza, España) y su relación con la bioestratigrafía del área. *Boletin del Instituto Geológico y Minero de España*, 78:187-373.

Dehm, R. 1935. Über tertiäre Spaltenfüllungen im Fränkischen und Schwäbischen Jura. *Abhandlungen der Bayerischen Akademie der Wissenschaften, mathematish-naturwissenschaftliche Klasse, Abteilung*, 29:1-86.

Dehm, R. 1950. Die Nagetiere aus dem Mittel-Miozän (Burdigalium) van Wintershof-West bei Eichstätt in Bayern. *Neues Jahrbuch für Mineralogie, Geologie und Paläontologie, Abhandlungen, B*, 91, 3: 321-428.

Díaz, M. and López, N. 1979. El Terciario continental de la Depresión Intermedia (Cuenca). Bioestratigrafía y Paleogeografía. *Estudios Geológicos*, 35:149-167.

Freudenberg, H. 1941. Die oberoligocänen Nager von Gaimersheim bei Ingolstadt und ihre Verwandten. *Palaeontographica, 92, A*:99-164.

Freudenthal, M. 1996. The Early Oligocene rodent fauna of Olalla 4A (Teruel, Spain). *Scripta Geologica*, 112:1-67.

Freudenthal, M. 2004. Gliridae (Rodentia, Mammalia) from the Eocene and Oligocene of the Sierra Palomera (Teruel, Spain). *Treballs del Museu de Geologia de Barcelona*, 12:97-173.

Freudenthal, M. and Martín-Suárez, E. 2006. Gliridae (Rodentia, Mammalia) from the late Miocene fissure filling Biancone 1 (Gargano, province of Foggia, Italy) *Palaeontologia Electronica*, 9, 2:1-23.

Freudenthal, M. and Martín-Suárez, E. in press. Revision of the subfamily Bransatoglirinae (Gliridae, Rodentia, Mammalia). *Scripta Geologica*, 135.

Friant, M. 1953. Une faune du Quaternaire ancien en France Méditerranéenne (Sète, Herault). *Annales Société Géologique du Nor*d, 73:161-170.

Hartenberger J.L. 1965. *Gliravus robiacensis* n. sp., nouveau Rongeur (Gliridae) de l'Eocène supérieur de Languedoc. Comptes Rendues sommaires Société Géologique de France, 1965:326-327.

Heller, F. 1930. Eine Forest-Bed-Fauna aus der Sackdillinger Höhle (Oberpfalz). *Neues Jahrbuch für Mineralogie, Geologie und Paläontologie, B, Beilageband*, 63:247-298.

Hugueney, M.1967. Les Gliridés (Mammalia, Rodentia) de l'Oligocène supérieur de Coderet-Branssat (Allier). *Comptes Rendus sommaires Société Géologique de France*, 1967:91-92.

Hugueney, M. 1969. Les rongeurs (Mammalia) de l'Oligocène supérieur de Coderet-Bransat (Allier). *Documents du Laboratoire de Géologie de la Faculté des Sciences de Lyon*, 34:1-227.

Hugueney, M., Adrover, R., and Moissenet, E. 1985. *Gliravus bravoi* nov. sp., la plus grande espèce du genre *Gliravus* (Mammalia, Rodentia, Gliridae) dans l'Oligocène supérieur d'Espagne. *Géobios*, 18, 2:251-256.

Kretzoi, M. 1959. Insectivoren, Nagetiere und Lagomorphen der jungstpliozänen Fauna von Csarnóta im Villányer Gebirge (Südungarn). *Vertebrata Hungarica*, 1:137-246.

Linnaeus, C. 1766. *Systema naturae sive regna tria naturae, secundum classes, ordines, genera, species,cum characteribus, differentiis, synonymis,locis.* Laurentii Salvii, Holmiae. Systema Naturae ed. 12:1-532.

López, N. 1977. In: López Martínez, N., Sesé Benito, C., and Sanz García, J.L. La microfauna (Rodentia, Insectivora, Lagomorpha y Reptilia) de las fisuras del Mioceno medio de Escobosa de Calatañazor. --- Trabajos Neógeno Cuaternario, 8:47-73.

Martín-Suárez, E. and Freudenthal, M. 2007. Gliridae (Rodentia, Mammalia) from the late Miocene fissure filling Rinascita 1 (Gargano, prov. Foggia, Italy). *Treballs del Museu de Geologia de Barcelona*, 14:37-59.

Mayr, H. 1979. Gebissmorphologische Untersuchungen an miozänen Gliriden (Mammalia, Rodentia) Süddeutschlands. *Thesis University Munich*:380 pp.

Mein, P. and Michaux, J.J. 1970. Un nouveau stade dans l'évolution des rongeurs pliocènes de l'Europe sud-occidentale. *Comptes Rendus des Séances de l'Académie des Sciences de Paris, D*, 270: 2780-2783.

Misonne, X. 1957. Mammifères Oligocènes de Hoogbutsel et Hoeleden. *Bulletin de l'Institut Royal des Sciences Naturelles de Belgique*, 33, 51:1-15.

Pallas, P.S. 1778. Novae species quadrupedum e glirium ordine, cum illustrationibus variis complurium ex hoc ordine animalium. --- Walther, Erlangen, I-VIII, 1-388.

Peláez-Campomanes, P. 2000. Mammalian faunas from the Paleogene of the Sierra Palomera (Teruel, Spain). *Journal of Paleontology*, 74,2:336-348.

Pomel, A. 1853. Catalogue méthodique et descriptif des vertébrés fossiles découverts dans le bassin hydrographique supérieur de la Loire et surtout dans la vallée de son affluent principal, l'Allier. *J.B. Baillière, Paris*:1-193.

Stehlin, H.G. and Schaub, S. 1951. Die Trigonodontie der simplicidentaten Nager. *Schweizerische Paläontologische Abhandlungen*, 67:1-385.

Thaler, L. 1966. Les rongeurs fossiles du Bas-Languedoc dans leurs rapports avec l'histoire des faunes et la stratigraphie du Tertiaire d'Europe. *Mémoires de Muséum National d'Histoire Naturelle, C*, 17:1-295.

Ünay, E. 1989. Rodents from the Middle Oligocene of Turkish Thrace. *Utrecht Micropaleontological Bulletins, Special Publication*, 5:1-119.

Ünay, E. 1994. Early Miocene rodent faunas from the eastern Mediterranean area. Part IV. The Gliridae. *Proceedings Koninklijke Nederlandse Akademie van Wetenschappen*, 97, 4:445-490.

van der Meulen, A.J. and de Bruijn, H. 1982. The mammals from the Lower Miocene of Aliveri (Island of Evia, Greece). Part 2: The Gliridae. *Proceedings Koninklijke Nederlandse Akademie van Wetenschappen, B*, 85, 4:485-524.

Vianey-Liaud, M. 1989. Parallelism among Gliridae (Rodentia): the genus *Gliravus* Stehlin & Schaub. *Historical Biology*, 2:213-226.

Vianey-Liaud, M. 1994. La radiation des Gliridae (Rodentia) à l'Eocène supérieur en Europe Occidentale et sa descendance Oligocène. *Münchner Geowissenschaftliche Abhandlungen, A*, 26:117-160.

Vianey-Liaud, M. 2004. Gliridae (Mammalia, Rodentia) de l'Oligocène européen. Origine de trois genres miocènes. *Coloquios de Paleontología, Volumen Extraordinario* 1:669-698.

Zammit Maempel, G. and de Bruijn, H. 1982. The Plio/Pleistocene Glirids from the Mediterranean Islands reconsidered. *Proceedings Koninklijke Nederlandse Akademie van Wetenschappen, B*, 85, 1:113-128.